13th World Conference on Earthquake Engineering
Vancouver, B.C., Canada
August 1-6, 2004
Paper No. 1863

Evaluations of 1D Simple Structural Models for 2D Steel Frame Structures

Hiroyuki TAGAWA[1], Gregory MACRAE[2], and Laura LOWES[3]

SUMMARY

The ability of a number of 1D simple structural models to represent the behavior of 2D ductile steel moment frames is discussed. The 1D models include (1) a bilinear single-degree-of-freedom (SDOF) model, (2) a multi-linear SDOF model, (3) a bilinear multi-degree-of-freedom (MDOF) shear-beam model, (4) a multi-linear MDOF shear-beam model, and (5) a coupled shear-flexural-beam model. The seismic performance of these models is evaluated using a number of ground motions. It is shown that bilinear SDOF and MDOF shear-beam models tend to have excessively large interstory displacements if the structure possesses a large lateral force reduction factor and a negative post-yield tangent stiffness due to P-Δ effects or material strength degradation. The tendency for large drifts is reduced if (1) a bilinear hysteretic loop is modified to be multi-linear or if (2) a flexural-beam (continuous column) is combined with the MDOF shear-beam models. Finally, it is shown that 2D steel moment ductile frames can be represented by 1D MDOF models consisting of the shear-beams coupled with a flexural-beam.

INTRODUCTION

In the 1994 Northridge Earthquake and the 1995 Kobe Earthquake, a number of steel moment structures suffered severe damage particularly at many beam-column welded connections. However, none or few of them completely collapsed during the earthquakes (Nakashima et al, 1997). These severely-damaged but non-collapsed structures might be considered to possess some elements to resist seismic and gravity loading after other elements are severely damaged and lost their resistance (Iyama and Kuwamura, 1999). The redundancy of structures may play an important role particularly for damage states near the structural collapse condition. For the economic design of new structures and a reliable evaluation of old structures, the redundant characteristics that the structures are likely to possess should be considered reasonably in structural modeling. Simplified structural models with reduced D.O.F.s such as SDOF and

[1] Ph.D. Candidate, Department of Civil and Environmental Engineering, University of Washington, Seattle, USA. Email: htagawa@u.washington.edu
[2] Associate Professor, Department of Civil and Environmental Engineering, University of Washington, Seattle, USA. Email: macrae@u.washington.edu
[3] Assistant Professor, Department of Civil and Environmental Engineering, University of Washington, Seattle, USA. Email: lowes@u.washington.edu

MDOF shear-beam models often used in structural preliminary design or evaluation may poorly represent the structural behavior.

A number of researchers have investigated the structural redundancy of indeterminate structures under static loading (e.g. Fu and Moses, 1989, Frangopol and Curley, 1987). Recently, several researchers (e.g. Bertero and Bertero, 1999, Wen and Song, 2003) have attempted to define, quantify and evaluate the structural redundancy under earthquake dynamic loading. Iyama and Kuwamura (1999) described the redundant performance of steel braced moment frames using SDOF models consisting of two coupled elastic–perfectly plastic (EPP) SDOF oscillators with different natural frequencies. It was observed that, although the system has an initial natural frequency close to the predominant frequency of ground motion and one oscillator is severely damaged, the other oscillator with a different natural frequency and displacement ductility capacity provides resistance to the system. This redundancy, created by dual framing, may be related to the "flexible – stiff mixed framing concept" described by Akiyama (1985) and Takahashi and Akiyama (1997). In these studies, the advantages of flexible – stiff mixed framing were explained in terms of an energy absorption efficiency using MDOF shear-beam models consisting of two EPP shear-beam models with long or short natural periods. It was shown that a system of elements with different natural periods performed well since a flexible element did not yield and provided the "origin-orientating" restoring force to the system after a stiff element yielded. This research demonstrated clear advantages of dual framing systems in terms of redundancy by parametric analyses using simple structural models. However, relationships between the responses of simple structural models and those of more realistic 2D frame models were not clearly presented. Moreover, the hysteretic loops assumed in their simple models are EPP. Redundant structural characteristics may play more significant role when some elements are degraded during an earthquake.

In this study, the seismic dynamic response of five different types of simple structural models, which are referred to as "1D" models since they have only horizontal D.O.F.s in one direction, are evaluated and compared to each other. They are (1) a bilinear SDOF model, (2) a multi-linear SDOF model, which may be similar to the model used by Iyama and Kuwamura (1999), (3) a bilinear multi-degree-of-freedom (MDOF) shear-beam model, (4) a multi-linear MDOF shear-beam model, which may be similar to the model used by Takahashi and Akiyama (1997), and (5) a coupled shear-flexural-beam model, which is introduced in this study. The post-yield stiffness ratio of the hysteretic loops is varied in this study. Also, 2D steel ductile moment frame responses are related to 1D structural model responses. The aims of this study are to answer the following questions:

- How do bilinear SDOF or MDOF shear-beam models with a negative post-yield tangent stiffness perform during earthquake motions?
- How does the modification of bilinear hysteretic loops to multi-linear loops with extended positive stiffness regions affect the structural performance of SDOF and MDOF structures?
- How does the addition of a flexural-beam (continuous column) affect the seismic performance of a MDOF shear-beam model with a negative tangent stiffness ratio?
- How are 2D steel ductile moment frame structures related to 1D structural models? How do 2D steel ductile moment frame form the redundant mechanism of resisting lateral forces?

BACKGROUND OF POST-YIELD STIFFNESS EFFECTS ON STABILITY

Under earthquake dynamic loading, a post-yield tangent stiffness of the structure may have significant impacts on the displacements if the structure possesses relatively low strength and if moderate or severe yielding occurs (Jennings and Husid, 1968, Husid 1969). The mathematical background on the effects of post-yield tangent stiffness on the structural stability is summarized below. The incremental equation of motion for SDOF structure is given by Equation 1, where m is a mass, c is a viscous damping ratio, and $k(t)$ is an instantaneous tangent stiffness, $\ddot{u}_g$ is a ground motion acceleration, and Δt is a time increment.

$$m(\Delta\ddot{u}) + c(\Delta\dot{u}) + k(t)\cdot(\Delta u) = -m(\Delta\ddot{u}_g) \qquad \text{(Equation 1)}$$

A displacement of the structure, u, are a sum of the small displacement increments during a small time-step, Δu, and given by Equation 2.

$$u = \Sigma(\Delta u) = \Sigma(\Delta u_P + \Delta u_H) \qquad \text{(Equation 2)}$$

where, Δu_P is a particular solution of the incremental displacement and it is usually small except for the case of resonance (Araki and Hjelmstad, 2000). Δu_H is a homogenous solution (i.e. solution for free vibration) given by Equations 3, 4, and 5 (Chopra, 2001).

(a) $4\cdot k(t)m - c^2 > 0$:

$$\Delta u_H = C_1\cdot\exp\left(\frac{-c}{2m}\Delta t\right)\cdot\cos\left(\frac{\sqrt{4km-c^2}}{2m}\Delta t\right) + C_2\cdot\exp\left(\frac{-c}{2m}\Delta t\right)\cdot\sin\left(\frac{\sqrt{4km-c^2}}{2m}\Delta t\right)$$

(Equation 3)

(b) $4\cdot k(t)m - c^2 = 0$:

$$\Delta u_H = C_1\cdot\exp\left(\frac{-c}{2m}\Delta t\right) + C_2\cdot\Delta t\cdot\exp\left(\frac{-c}{2m}\Delta t\right)$$

(Equation 4)

(c) $4\cdot k(t)m - c^2 < 0$:

$$\Delta u_H = C_1\cdot\exp\left(\frac{-c+\sqrt{c^2-4km}}{2m}\Delta t\right) + C_2\cdot\exp\left(\frac{-c-\sqrt{c^2-4km}}{2m}\Delta t\right)$$

(Equation 5)

where C_1, C_2 are determined by the initial conditions in each time increment. Case (a) gives an oscillatory displacement represented by a sinusoidal function since $\exp(-c\cdot\Delta t/2m)$ decays as Δt increases. Damping c is usually small for the structures with no viscous dampers, so let's assume that c is 0 for simplicity. Case (b) gives a gradual increase due to a term of Δt. Case (c) occurs when $k(t) < 0$. Case (c) gives a divergent drift increase in 1-direction represented by an exponential function since $\{-c + \sqrt{c^2 - 4km}\}/2m\cdot\Delta t$ is positive. This negative tangent stiffness, $k(t) < 0$, is not a necessary condition for large drifts in 1-direction during an earthquake motion since mass inertial and viscous damping forces affect the dynamic behavior and also a negative tangent stiffness may change to positive due to unloading during an earthquake motion (Bernal, 1998, Araki and Hjelmstad, 2000). This argument is applicable to MDOF structures. For MDOF structures, an eigenvalue of mass and instantaneous stiffness matrices, Ω_n, which is a square of the instantaneous frequency of the n^{th}-mode shape (i.e. $\Omega_n = \omega_n^2$), corresponds to the instantaneous tangent stiffness divided by the mass in SDOF structures.

1D SIMPLE STRUCTURAL MODEL RESPONSES

Five different 1D simple structural models are used to evaluate their seismic performance particularly from the perspective of the stability and redundancy. To investigate collapse potential, the models are used to predict response under multiple ground motion records and model post-yield stiffnesses are adjusted. The 40 SAC NF records are used to consider the impact of ground motion variability (Somerville et al. 1997).

Bilinear SDOF or MDOF Shear-beam Models

Bilinear SDOF models and bilinear MDOF shear-beam model, in which bilinear SDOF models are built up, are illustrated in Figure 1(a) and Figure 1(b). A stiffness matrix of a MDOF shear-beam model, $[K_s]$, is banded and given by Equation 6, where k_n is a stiffness of the n^{th} story. This banded type matrix has an unique characteristics represented by Equation 7 (Tagawa, 2004), where $\Omega_1, \Omega_2, \cdots, \Omega_n$ are eigenvalues of the stiffness matrix, $[K_s]$. As this equation implies, the number of negative story stiffnesses, k, is same to the number of negative eigenvalues, Ω; for example, if only one of story stiffness values is negative, only one of the eigenvalues is negative.

$$[K_s] = \begin{bmatrix} k_1 + k_2 & -k_2 & 0 & \cdots & 0 \\ -k_2 & k_2 + k_3 & \ddots & \ddots & \vdots \\ 0 & \ddots & \ddots & \ddots & 0 \\ \vdots & \ddots & \ddots & k_{n-1} + k_n & -k_n \\ 0 & \cdots & 0 & -k_n & k_n \end{bmatrix} \quad \text{(Equation 6)}$$

$$k_1 k_2 k_3 \cdots k_n = \Omega_1 \Omega_2 \Omega_3 \cdots \Omega_n \quad \text{(Equation 7)}$$

Bilinear SDOF and MDOF shear-beam models are analyzed for SAC NF ground motions. Parameters used are as follows.

1. In the bilinear SDOF models, the natural period of the model is defined to be 1.285s, the value estimated by the IBC (2000) code for a 9-story steel frame with a fixed lateral force reduction factor, $R = 4$.
2. For the SDOF models, a post-yield tangent stiffness ratio is defined as r-θ, where r accounts for material non-linearity and θ is the 1st-order approximation of P-Δ effects with $\theta = P/(KH)$, where P is a weight, K is an initial stiffness, and H is a height.
3. For bilinear MDOF shear-beam models, the 1st natural period including P-Δ effects, T_p, is 1.285s.
4. For bilinear MDOF models, the post-yield stiffness for story s is defined r_s-θ_s, where r_s accounts for material post-yield stiffness for story, s, and θ_s is the P-Δ stability coefficient for story, s. $\theta_s = \Sigma P/K_s H_s$, where ΣP is a weight from above stories, K_s is a story initial stiffness, and H_s is a story height. For simplicity, $r_s - \theta_s$ for all stories are assumed to be same in this study.

The results of the incremental dynamic analyses (Vamvatsikos and Cornell, 2002) using the bilinear SDOF models with r-θ = 0.06, 0.03, 0, -0.03, and -0.06 to the NF17 record are presented in Figure 2. It is found that the drift increases for r-θ = -0.06 or -0.03 rapidly after seismic demand represented by elastic spectral acceleration at the natural period, S_A, becomes greater than 1.5g. This unstable behavior is due to a negative post-yield tangent stiffness. Next, for bilinear MDOF shear-beam model with various r_s-θ_s, the dynamic analyses are carried out using 20 SAC NF-SN (strike-normal) records as shown in Figure 3, where peak story drift ductility responses in these models are plotted as a function of post-yield stiffness. It can be observed that when $(r_s - \theta_s)$ are positive, median values of the peak drift are relatively stable and fall between the drifts estimated by the Equal Displacement Method (EDM) or the Equal Energy Method (EEM). However, when $(r_s - \theta_s)$ becomes negative, the peak drifts are excessively large, and the bilinear MDOF shear-beam model indicates a high probability of structural collapse. From the perspectives of the redundancy, it can be said that bilinear MDOF shear-beam model with a negative tangent stiffness is a weak link non-redundant system (Achintya and Sankaran, 2000).

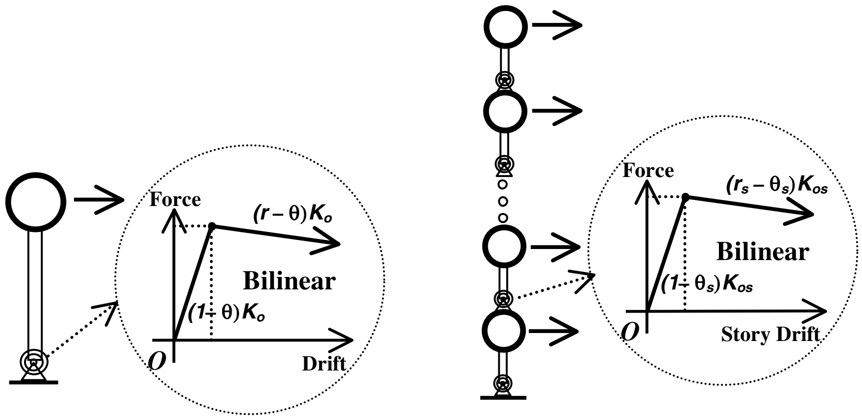

(a) Bilinear SDOF **(b) Bi-linear MDOF Shear-beam**

Figure 1: 1D bilinear SDOF or MDOF shear-beam models.

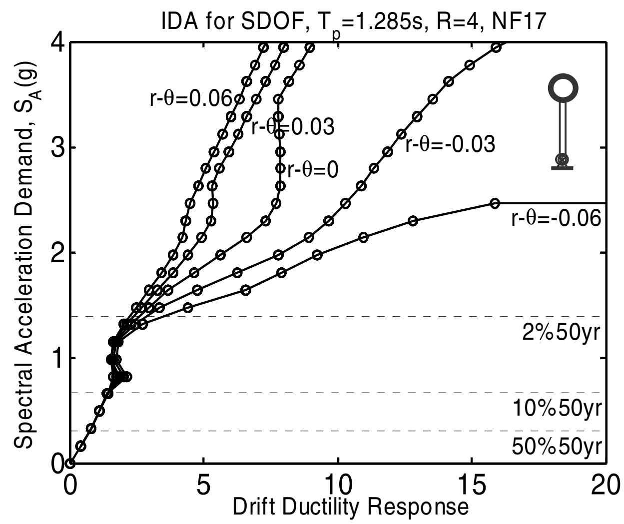

Figure 2: Peak drift ductility response in bilinear SDOF model corresponding to various *r*-θ.

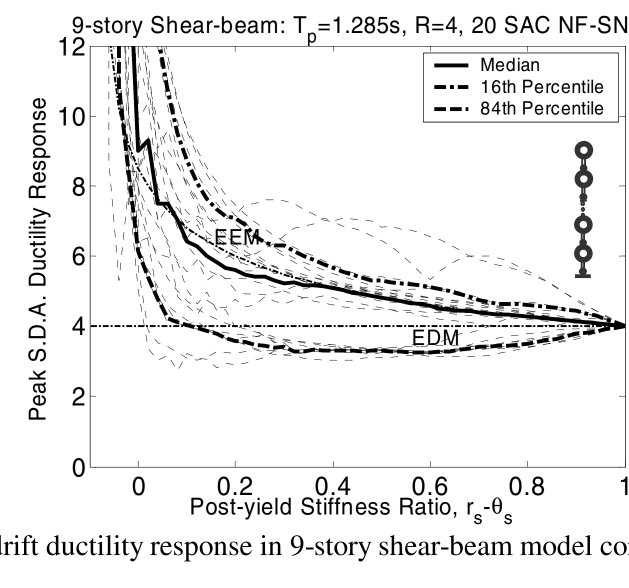

Figure 3: Peak story drift ductility response in 9-story shear-beam model corresponding to various r_s-θ_s.

Multi-linear SDOF or MDOF Shear-beam Model

A tri-linear SDOF model, in which multiple bilinear SDOF models are connected with perfectly-rigid links, and tri-linear MDOF shear-beam models, in which multiple bilinear shear-beams are connected with perfectly-rigid links, are illustrated in Figure 4(a) and Figure 4 (b). The stiffness matrix of the tri-linear MDOF shear-beam model is banded in a same way as for the bilinear shear-beam model given by Equation 8, where k_{As}, k_{Bs} represent the Oscillators A and B (which have different yield displacements and consist of tri-linear system) stiffness values in the s^{th}-story. As seen in the matrix form, although a tangent stiffness of Oscillator A (i.e. k_{As}) becomes negative, there is a possibility that the tangent stiffness of Oscillator B (i.e. k_{Bs}) remains positive and provides positive stiffness to that story. In this case, the displacements may be reduced due to delayed positive slope region in the story hysteretic loops.

$$[K] = \begin{bmatrix} \sum_{i=A}^{B}(k_{i1}+k_{i2}) & -\sum_{i=A}^{B}k_{i2} & 0 & \cdots & 0 \\ -\sum_{i=A}^{B}k_{i2} & \sum_{i=A}^{B}(k_{i2}+k_{i3}) & \ddots & \ddots & \vdots \\ 0 & \ddots & \ddots & \ddots & 0 \\ \vdots & \ddots & \ddots & \sum_{i=A}^{B}(k_{i(n-1)}+k_{i(n)}) & -\sum_{i=A}^{B}k_{i(n)} \\ 0 & \cdots & 0 & -\sum_{i=A}^{B}k_{i(n)} & \sum_{i=A}^{B}k_{i(n)} \end{bmatrix} \quad \text{(Equation 8)}$$

To evaluate multi-linear hysteretic loop effects, tri-linear SDOF and MDOF shear-beam models are developed and analyzed. Parameters used to describe tri-linear hysteretic loops are the 1st yield strength reduction factor, α_{tri}, and a yield displacement amplification factor, β_{tri}, in conjunction with bilinear loops as shown in Figure 4-a. In the models used for this study, α_{tri} is 0.5, and β_{tri} is 2, 3, 4, and 5. The bilinear models that are modified for the tri-linear study have T = 1.285s, R or R_s = 4 with post-yield tangent stiffness ratio, r or r_s of -0.06 (let $\theta = 0$, $\theta_s = 0$). Figure 5 shows the results of the incremental dynamic analyses for bilinear or tri-linear SDOF models using scaled NF17 records (Somerville et al. 1997). It has been observed that the tri-linear models with β_{tri} = 3, 4, 5 have smaller peak drifts than the bilinear model or the model with β_{tri} = 2 as the ground motion demand represented by S_A increases. Next, Figure 6 shows the peak story drifts in the bilinear or tri-linear MDOF shear-beam models analyzed for the 40 SAC NF records. From this data it can be observed that the tri-linear models have smaller peak drifts than the bilinear models. This is a multi-hysteretic loop effect with an extended positive slope region at the expense of a decrease in strength. From the perspective of the redundancy considering the possibilities of simultaneous events, it may be said that a multi-linear MDOF shear beam is parallel system at a story-level and this model tends to be more redundant than a bilinear MDOF shear beam. However, after the peak strength, this model is still a weak link system along the building height.

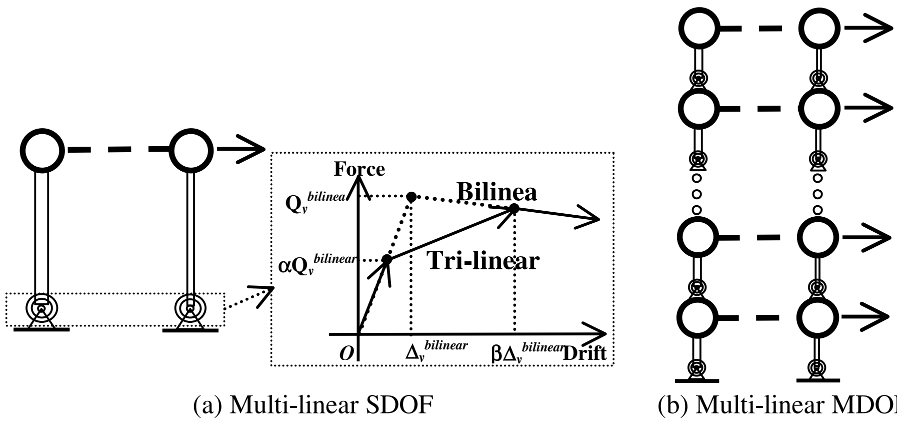

Figure 4: 1D Multi-linear SDOF or MDOF shear-beam models.

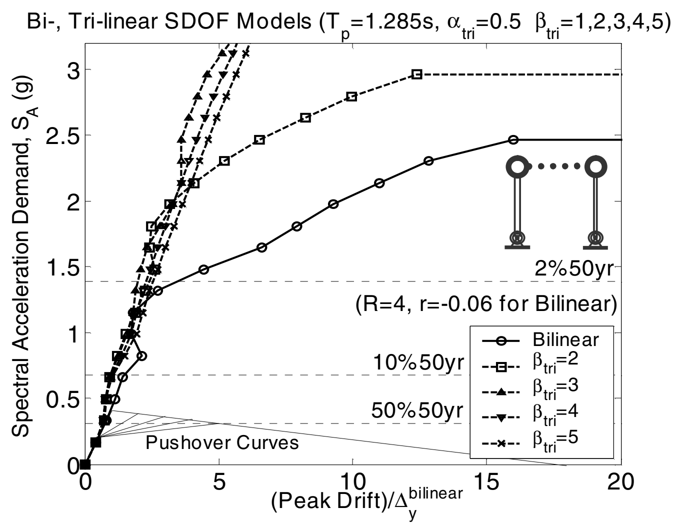

Figure 5: Peak drift ductility responses in bilinear or tri-linear SDOF models with $R_{bi} = 4$, $r_{bi} = 4$, and $\alpha_{tri} = 0.5$, $\beta_{tri} = 1, 2, 3, 4, 5$ for incrementally-scaled NF17 records.

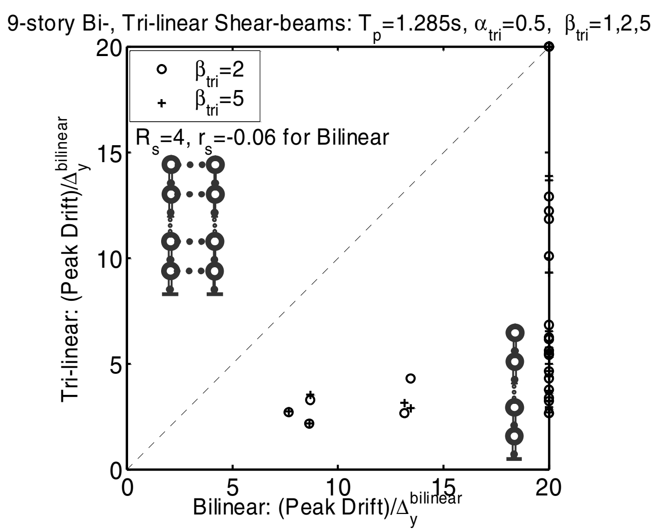

Figure 6: Peak drifts in bilinear or tri-linear SDOF or MDOF shear-beam models for 40 NF records.

1D Coupled Shear-flexural-beam Model

A 1D coupled shear-flexural-beam model, in which the MDOF shear-beam is connected to a flexural beam (continuous column) with perfectly rigid links, is illustrated in Figure 7. This is different from the models developed and analyzed by Wada and Huang (1995), in which a flexural-beam is considered to model the horizontal deformation by column axial deformations. The flexural-beam model used in this study follows a definition presented by Chopra (2000) and its deformation is same as the frame deflection with no beam stiffness without column axial deformation. The moment distribution along the flexural-beam is continuous since there is no moment input from the beams at the nodes as illustrated in Figure 8(a). An incremental equation of motion for the coupled shear-flexural-beam model is given by Equation 9, where $[K_s]$ or $[K_f]$ are stiffness matrices of the shear-beam part or the flexural-beam part.

$$[M]\{d\ddot{\Delta}\} + [C]\{d\dot{\Delta}\} + ([K_s] + [K_f])\{d\Delta\} = -[M]\{d\ddot{\Delta}_g\} \qquad \text{(Equation 9)}$$

The shear-beam matrix, $[K_s]$, is given by Equation 6. The flexural-beam matrix, $[K_f]$, is obtained as follows. For each beam element as illustrated in Figure 8(b), the governing equation is given by Equation 5.

$$\begin{Bmatrix} F_i^a \\ M_i^a \\ F_i^b \\ M_i^b \end{Bmatrix} = [K_i^{element}] \begin{Bmatrix} \Delta_i^a \\ \theta_i^a \\ \Delta_i^b \\ \theta_i^b \end{Bmatrix} \qquad \text{(Equation 10)}$$

For a whole flexural-beam as illustrated in Figure 8(c), the governing equation is given by Equation 11 separating displacement (force) or rotational (moment) terms, where $\{F_{total}\} = \{F_0, \ldots, F_n\}$, $\{M_{total}\} = \{M_0, \ldots, M_n\}$, $\{\Delta_{total}\} = \{\Delta_0, \ldots, \Delta_n\}$, and $\{\theta_{total}\} = \{\theta_0, \ldots, \theta_n\}$.

$$\begin{Bmatrix} \{F_{total}\} \\ \{M_{total}\} \end{Bmatrix} = \begin{bmatrix} [K_{\Delta\Delta}] & [K_{\Delta\theta}] \\ [K_{\theta\Delta}] & [K_{\theta\theta}] \end{bmatrix} \begin{Bmatrix} \{\Delta_{total}\} \\ \{\theta_{total}\} \end{Bmatrix} \qquad \text{(Equation 11)}$$

A flexural beam is subject to only lateral forces from the links at the nodes, then $\{M_{total}\} = 0$. As a result, a stiffness matrix of the flexural-beam only in terms of node displacements is obtained.

$$[K_f] = \{F_{total}\}/\{\Delta_{total}\} = [K_{\Delta\Delta}] - [K_{\Delta\theta}][K_{\theta\theta}]^{-1}[K_{\theta\Delta}] \qquad \text{(Equation 12)}$$

A matrix of a coupled shear-flexural-beam model, $[K_{sf}] = [K_s] + [K_f]$, is fully populated and this matrix form implies a story restoring force characteristics affected by the other story displacements.

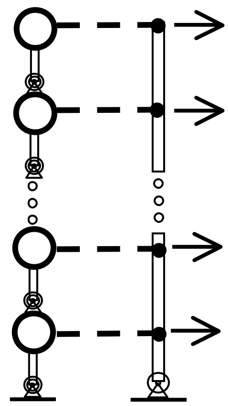

Figure 7: 1D coupled shear-flexural-beam model.

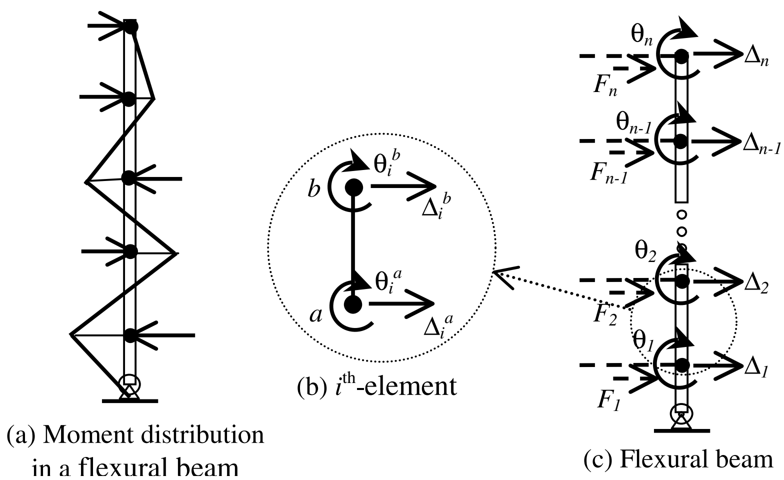

Figure 8: Flexural-beam in 1D coupled shear-flexural-beam model.

To consider the flexural-beam (continuous column) effects, a coupled shear-flexural-beam model is analyzed with various flexural-beam stiffness values. The shear-beam part in this model is unchanged from the above analyses. In this study, the flexural-beam is assumed to be elastic and attached to the ground with a pin. Figure 9 shows the story drift distributions corresponding to various flexural-beam stiffnesses in the 9-story coupled shear-flexural-beam model subject to NF17 record. It can be observed that the addition of the flexural-beam from the $\alpha_{c.c.} = (EI_{fi}/H^3) / K_{oi} = 0$ to 0.1 changes the drift distributions significantly; if no flexural-beam is added, the shear-beam has excessively large displacements (collapses). However, the flexural-beam is added, the drifts are distributed more uniformly. For an infinitely stiff flexural-beam, the drifts at each story are identical. This observation is similar to those obtained by MacRae et al. (2003) for braced steel frames with the continuous columns. Figure 10 shows the 1st story hysteretic loops of the shear-beam part, flexural-beam part, and their sum during the NF17 record. It can be observed that the flexural-beam part often recovers the negative post-yield stiffness of the shear-beam part and then the 1st story hysteretic loops have often positive values, which prevents the large 1-directional drift. The story post-yield stiffness increase due to the flexural-beam depends on the time-dependent deformation mode of the structure and it is not constant during an earthquake motion. To consider the time-dependent characteristics, eigenvalues of mass and stiffness matrices in the shear- and flexural-beams, Ω, are evaluated in Figure 11. Assuming that all stories yield over the height, the eigenvalues for the 1st, 2nd, and 3rd modes are calculated as a function of the flexural-beam stiffness ratio.

As seen in the figure, as $\alpha_{c.c.}$ increases from 0 to 0.02, the smallest 3 eigenvalues increase significantly. After that, the 1^{st} and 2^{nd} eigenvalues do not increase much, although the 3^{rd} (or higher) eigenvalue increases. Figure 12 shows the 1^{st} story drift angle histories for the coupled shear-flexural-beam models with the $\alpha_{c.c.}$ = 0, 0.02, and 0.2. It can be observed that the model with $\alpha_{c.c.}$ = 0 has excessively large drifts in 1-direction due to the negative eigenvalues. Also, a model with $\alpha_{c.c.}$ = 0.02 has a large 1-directional drift due to negative eigenvalues. In contrast, a model with $\alpha_{c.c.}$ = 0.2 has relatively small 1-directional drift since the flexural-beam provides positive stiffness to shear-beam model at almost time during the earthquake motion. These observations match the results shown in Figure 11. Therefore, it can be said that, even though a story in the shear-beam has a negative story tangent stiffness, the flexural-beam along the height may provide the positive stiffness to the story. From the perspective of the redundancy, a coupled shear-flexural-beam model is a parallel redundant system along the building height.

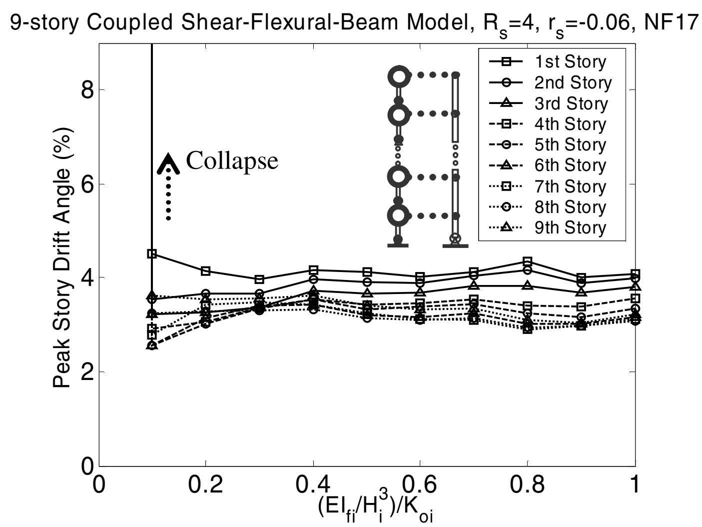

Figure 9: Peak story drift angle in 9-story coupled shear-flexural-beam models with various flexural-beam stiffnesses for NF17 record.

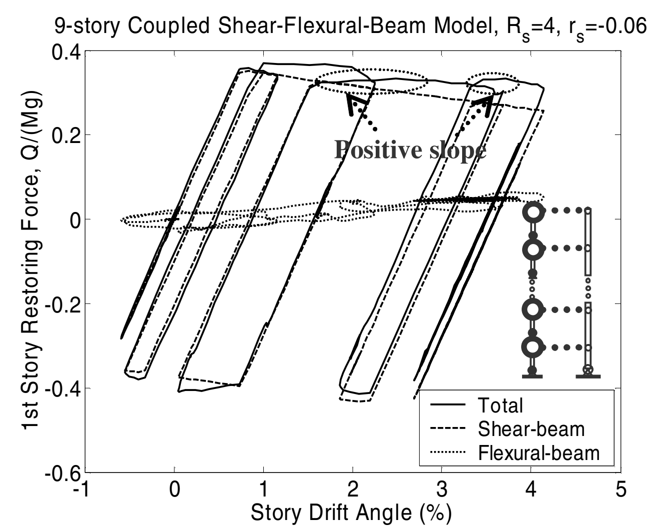

Figure 10: Hysteretic loops of the shear-beam, flexural-beam parts and a total of them in the 1^{st} story of 9-story coupled shear-flexural-beam model with R_s = 4, r_s = -0.06 and $\alpha_{c.c.}$ = 0.2 during NF17.

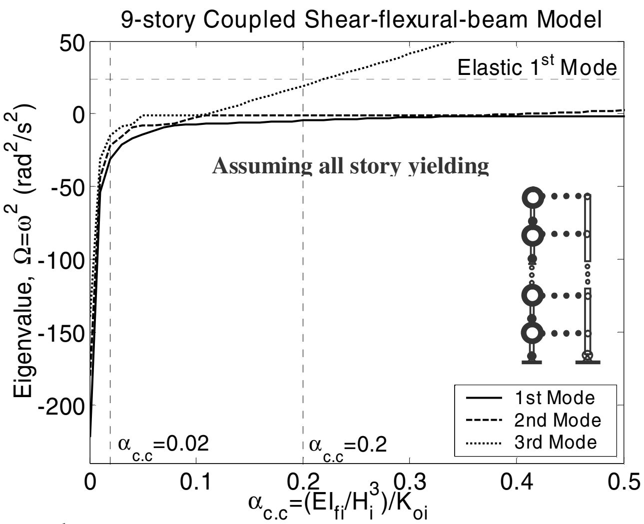

Figure 11: 1st, 2nd, and 3rd mode eigenvalues in the coupled shear-flexural-beam model with various stiffnesses assuming all story yield mechanism.

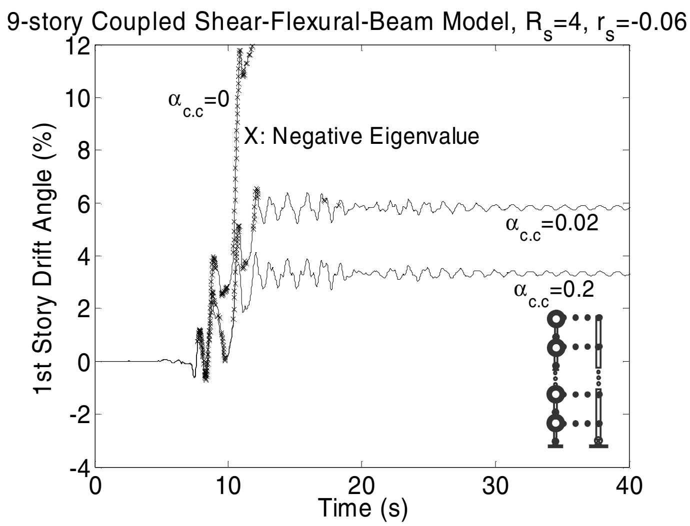

Figure 12: 1st story drift angle histories in 9-story coupled shear-flexural-beam model with $\alpha_{c.c.}$ = 0, 0.02, and 0.2) during NF17 record.

Next, in order to evaluate multi-linear hysteretic loop effects and the flexural-beam effects together, the systems of one or multiple shear-beams and a flexural-beam are analyzed for 40 SAC NF records discussed above. Bilinear and multi-linear shear-beam models are unchanged from those used in the above analyses. A flexural-beam stiffness ratio, $(EI_{fi}/H_i^3)/K_{oi}$ (where EI_{fi} is an i^{th}-story flexural stiffness of a flexural-beam, H_i is an i^{th}-story height, K_{oi} is an i^{th}-story shear-beam initial stiffness) is set at 0.3. The peak drifts in the systems are shown in Figure 13. It can be observed that the peak drifts in both models become similar due to a presence of the flexural-beam, and the effects of the flexural-beam on the hysteretic loop us more significant than making the hysteretic loop tri-linear.

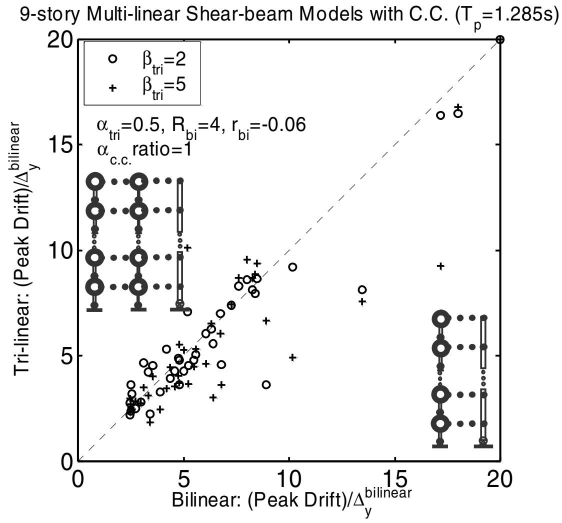

Figure 13: Peak drift ductility responses in 1D models of bilinear or tri-linear shear-beam plus a flexural-beam for 40 SAC NF records.

SIMPLIFICATION of 2D FRAMES to 1D COUPLED SHEAR-FLEXURAL-BEAM MODELS

If 2D frame responses can be decoupled into shear- and flexural-beam deformation modes, then 1D structural models considered previously can be used to predict the response of the 2D frame. An approach to decoupling shear- and flexural-beam modes for 2D frames is summarized in Figure 14. First, the model of the 2D moment frame is modified to that of a shear-beam structure by adding flexural pins at column mid-height. This model is referred to as the *pinned-column model*. Then, to incorporate column continuity in the original frame, a continuous column (C.C.), which can be modeled as flexural-beam in 1D models, is added to the *pinned-column frame*. This model is referred to as a *pinned-column frame with the C.C.* The C.C. stiffness is obtained so that the original (*no-pinned-column*) frame and the *pinned-column frame with the C.C.* have similar drift responses. Based on kinematics considerations, the *pinned-column frame with the C.C.* is similar to a 1D coupled shear-flexural-beam model with each SDOF model representing each story subassembly characteristics in the 2D *pinned-column frame*. Therefore, if an appropriate C.C. stiffness is available, 2D frames can be simplified to 1D simple structural models.

To assess this simplification approach, a 9-story 4-bay steel moment frame obtained from SAC steel structure project (Gupta and Krawinkler, 2000) is investigated. Figure 15 shows the static pushover analysis results for the original (*no-pinned-column*) frame and the *pinned-column frame with various the C.C.* flexural stiffness (C.C. ratio is a flexural-beam stiffness normalized by a sum of moment frame column stiffnesses). It has been observed that the *pinned-column frame with the C.C.* (C.C. ratio = 0.4) gives similar static responses to the original frame. Based on this simplification procedure, an equivalent 1D coupled shear-flexural-model is made for SAC 9-story steel moment frame. The 1D coupled shear-flexural-beam model corresponding to the *pinned-column frame with the C.C.* gives similar drifts to the original 2D frame until 10% S.D.A. as seen in Figure 16. Slight differences mainly come from the boundary conditions at the basement and different analysis time-steps used for two models. When the story subassembly in the bottom story is extracted from the shear-beam part, this has a large negative post-yield tangent stiffness ratio (approximately, -6%) due to P-Δ effects from a large weight from the above stories (Tagawa, 2004, Tagawa et al., 2004). However, a collapse does occur rarely. This is because the 2D moment frame has column continuity (flexural-beam effects). This fact implies that the actual 2D steel ductile moment frame tends to possess redundant mechanism of resisting lateral forces in a similar way that the flexural-beam plays in the 1D structural models.

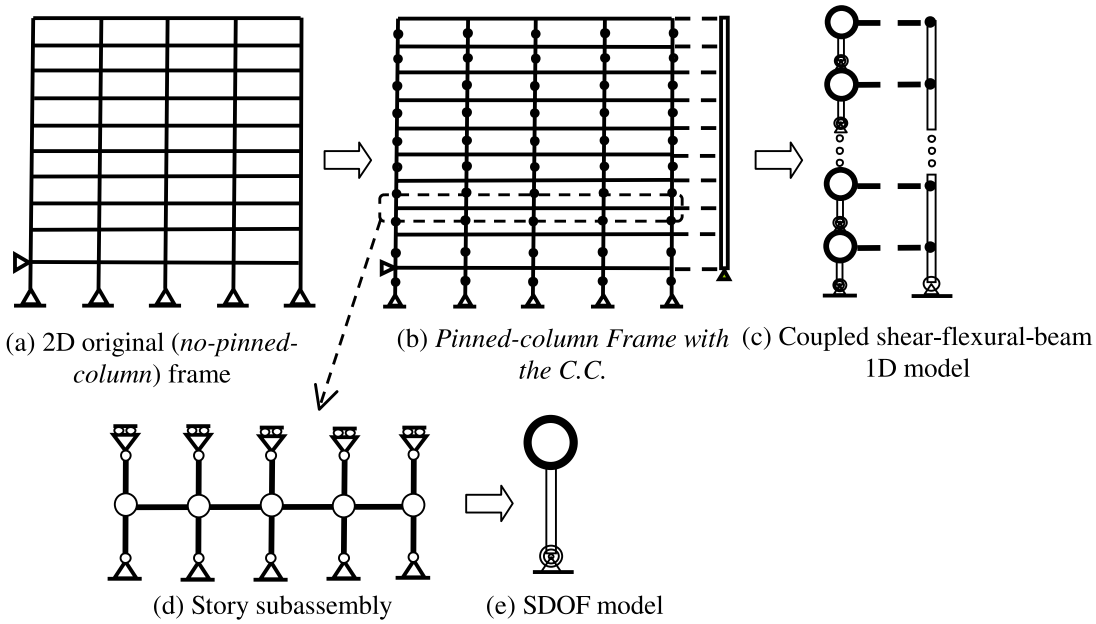

Figure 14: Simplification of 2D frame responses.

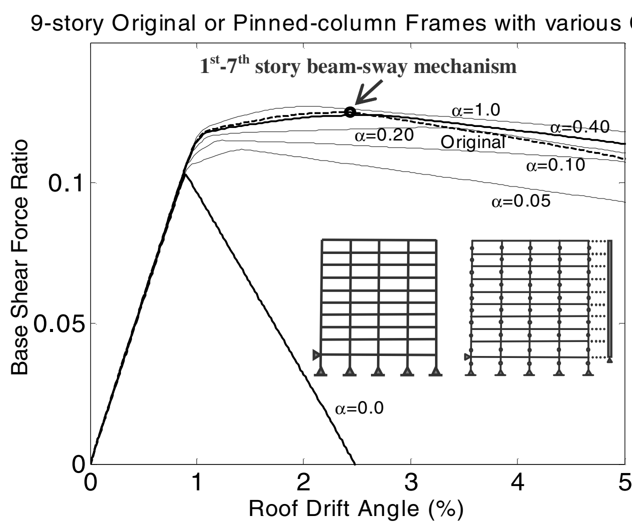

Figure 15: Pushover curves in 9-story SAC original (*no-pinned-column*) frame and the *pinned-column frames with the various C.C.*

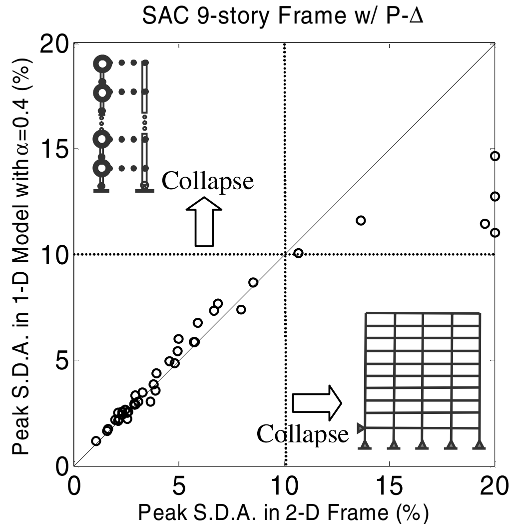

Figure 16: Peak story drift angles in 9-story SAC original frame and the equivalent 9-story coupled shear-flexural-beam model for 40 SAC NF records.

CONCLUSIONS

The seismic responses of 5 types of 1D structural models representing 2D steel moment frames are analyzed for many ground motions in this study to obtain better understanding of structural performance relating to stability and redundancy under earthquake dynamic loading. Major findings are:

1) SDOF and MDOF shear-beam models indicate a high likelihood of a structure exhibiting excessively large drifts when the structure has a negative tangent stiffness due to P-Δ effects. This is not usually seen in the actual 2D frames.
2) The modification of bi-linear hysteretic loops with a negative post-yield stiffness to multi-linear hysteretic loops with an extended positive slope region and smaller yield strength for both SDOF and MDOF shear-beam models tends to decrease the displacement demands and the possibility of collapse.
3) The addition of the flexural-beam (continuous column) to a MDOF shear-beam model with the negative tangent stiffness often decreases the displacements significantly. This is because a negative story tangent stiffness in a story (or eigenvalues of instantaneous stiffness matrix under inelastic deformation) is changed to positive due to the flexural-beam even with a small flexural stiffness.
4) A modeling approach that decouples the response of a 2D frame into shear- and flexural-beam deformation modes is proposed. If an appropriate stiffness of the flexural-beam is determined, 1D shear-beam model coupled with the flexural-beam can represent the inter-story or roof displacements of MDOF 2D moment frame structures well.

REFERENCES

1. Nakashima, M., Yamao, K., and Minami, T., "*Post-earthquake Analysis on Damage to Steel Beam-to-Column Connections Observed in The 1995 Hyogoken-Nanbu Earthquake*", Stability and Ductility of Steel Structures, Pergamon, 1998.
2. Iyama, J. and Kuwamura, H., "*Probabilistic Advantages of Vibrational Redundancy in Earthquake-resistant Steel Frames*", Journal of Constructional Steel Research 52, 1999.

3. Fu, G. and Moses, F., "*Probabilistic Concepts of Redundancy and Damage Tolerability*", Structural Safety and Reliability, Proceedings of the 5th ICOSSAR, 1989.
4. Frangopol, M. and Curley, P., "*Effects of Damage and Redundancy on Structural Reliability*", Journal of Structural Engineering, ASCE, 1987.
5. Bertero, R. and Bertero, V., "*Redundancy in Earthquake-resistant Design*", Journal of Structural Engineering, ASCE, January, 1999.
6. Wen, Y. and Song, S., "*Structural Reliability/Redundancy under Earthquakes*", Journal of Structural Engineering, ASCE, January, 2003.
7. Akiyama, H., "*Earthquake-resistance Limit-state Design for Buildings*", University of Tokyo Press, 1985.
8. Takahashi, M. and Akiyama, H., "*Damage Concentration Characteristics of Flexible–Stiff Mixed Shear-type Multi-story Frames under Earthquakes*", Journal of Structural and Construction Engineering, AIJ, No. 536, October, (in Japanese), 1997.
9. Jennings, P. and Husid, R., "Collapse of Yielding Structures under Earthquakes", Journal of Engineering Mechanics Division, ASCE, 94, 1968.
10. Husid, R. "The Effect of Gravity on the Collapse of Yielding Structures with Earthquake Excitation", Proceedings of the 4th WCEE, Santiago, Chile, 1969.
11. Araki, Y. and Hjelmstad K., "*Criteria for Assessing Dynamic Collapse of Elastoplastic Structural Systems*", Earthquake Engineering and Structural Dynamics, Vol. 29, 2000.
12. Chopra, A., "*Dynamics of Structures, Theory and Application to Earthquake Engineering*", 2nd edition, Prentice Hall, 2000.
13. Bernal, D., "*Instability of buildings during seismic response*", Engineering Structures, 20(4-6), 1998.
14. Somerville, P., et al., "*Development of ground motion time histories for phase 2 of the FEMA/SAC steel project*", Rep. No. SAC/BD97/04, SAC Joint Venture, Sacramento, California, 1997.
15. Tagawa, H., *Towards an Understanding of 3-D Structural Behavior*, Doctorate Thesis, Department of Civil Engineering, University of Washington, (to be completed), 2004.
16. ICBO., "*Uniform Building Code*", International Conference of Building Officials, Whittier, CA.
17. Vamvatsikos, D. and Cornell, A., "*Incremental Dynamic Analysis", Earthquake Engineering and Structural Dynamics*, Vol. 31, 3, 2002.
18. Achintya, and Sankaran, "Probability, Reliability and Statistical Methods in Engineering Design", John Willey & Sons, Inc., 2000.
19. Wada, A. and Huang, Y., "*Preliminary Seismic Design of Damage Tolerant Building Structures*", A New Direction in Seismic Design, Tokyo, 1995.
20. MacRae, G., Kimura, Y. and Roeder, C., "*Effect of Column Stiffness on Braced Frame Seismic Behavior*", Journal of Structural Engineering, ASCE, March, 2004.
21. Gupta, A. and Krawinkler, H., "*Seismic Demands for Performance Evaluation of Steel Moment Resisting Frame Structures*", John A. Blume Earthquake Engrg. Ctr. Rep. No. 132, Dept. of Civ. Engrg., Stanford University, CA, 1999.
22. Tagawa, H., MacRae, G., and Lowes, L., "Evaluation and Mitigation of P-Δ effects on 2D MDOF Frame Behavior", SSRC 2004 Annual Stability Conference, AISC, Long Beach, CA, 2004.